JOURNAL OF MATERIALS SCIENCE 30 (1995) 5502–5507

Measurement of elastic and anelastic properties of reaction-formed silicon carbide-based materials

A. WOLFENDEN, P. J. RYNN
Advanced Materials Laboratory, Mechanical Engineering Department, Texas A&M University, College Station, TX 77843, USA

M. SINGH
NASA Lewis Research Center, Cleveland, OH 44135, USA

The dynamic Young's modulus and the strain amplitude dependence of damping, at room temperature as well as at elevated temperatures, were determined for reaction-formed SiC (RFSC) ceramics, and the results are compared with those for other SiC materials. The method used was the piezoelectric ultrasonic composite oscillator technique (PUCOT). Five specimens were studied: NC 203 (a commercially produced SiC by Norton, Co.); RFSC No. 1 and RFSC No. 2 (each containing residual Si); RFSC No. 3 and RFSC No. 4 (both containing residual Si and $MoSi_2$). Metallographic observations showed that the microstructure of the RFSC is essentially isotropic with a uniform distribution of phases. The "rule of mixtures" calculations cannot be used to predict accurately the elastic modulus of the RFSC, but they can be used to predict the density to within 5%. It was determined that for the RFSC, the dynamic Young's modulus decreases as temperature increases, in a manner similar to that for other SiC materials. It was also found that the damping of the RFSC is generally independent of strain amplitude and is weakly affected by temperature. The activation energy was determined for the change in damping with change in temperature of RFSC No. 2 and RFSC No. 3.

1. Introduction

In recent years, there has been an increasing demand for high temperature ceramics and composite materials for high temperature structural applications. Silicon carbide-based ceramics and composites have attracted a great deal of attention due to their good strength and toughness, good creep and oxidation resistance, and high thermal conductivity [1–7]. The potential applications of these materials include components for advanced propulsion systems, heat exchanger and land-based turbines, automotive, and nuclear industries. Reaction-formed silicon carbide-based (RFSC) materials have many advantages over other silicon carbide materials produced by other techniques, i.e. hot pressing, hot isostatic pressing and sintering. Net shape or near-net shape components with complex shapes can be fabricated by the reaction forming technique. In addition, this process is capable of producing materials with tailorable microstructure and composition [4–7].

This work is part of continuing programs to determine the effect of various second phase constituents on the Young's modulus (elastic) and damping (anelastic) characteristics of RFSC materials. This study is limited to the silicon carbide materials with silicon and molybdenum disilicide as the second phases. The Young's modulus and damping characteristics of these materials have been measured as a function of temperature and compared with those of commercial silicon carbides.

2. Materials

RFSC materials used in the present study have been made by the reactive infiltration of a microporous carbon pre-form with molten silicon or a silicon–molybdenum alloy [4–7]. The final products are silicon carbide with some residual silicon or silicon carbide with molybdenum disilicide and silicon phases, with amounts depending on the alloy composition. The reactive infiltration can lead to complete conversion of carbon to a fully dense silicon carbide. However, in actual experimental conditions it is quite possible to have some residual free carbon and a little porosity in the final material. The presence of molybdenum disilicide in the final material has certain advantages. It has the brittle-to-ductile transition at temperatures ca. 1000 °C and this phenomenon allows it to act as a dispersed ductile phase at high temperatures.

Five different samples of SiC with various phases were investigated. The first specimen was NC 203, a commercially produced SiC manufactured by Norton, Co. This specimen contained no reinforcing phases. The other four specimens were reaction formed with different infiltrant compositions. Table I shows the identification of each specimen, the composition of the

0022–2461

TABLE I Volume fraction of reinforcing phases present in the RFSC, resulting from various infiltrants [4]

Specimen	Infiltrant	Volume fraction SiC	Volume fraction $MoSi_2$	Volume fraction Si
NC 203		1		
RFSC No. 1	Si	0.857		0.143
RFSC No. 2	Si	0.857		0.143
RFSC No. 3	Si–1.7 at % Mo	0.857	0.033	0.110
RFSC No. 4	Si–3.2 at % Mo	0.857	0.062	0.081

infiltrant and the approximate volume fractions of the residual phases.

3. Experimental procedure

The details of the specimen fabrication have been described elsewhere [4–7]. For metallographic studies, samples were cross-sectioned and polished. Specimens used for the Young's modulus and damping measurements were 50 mm long, 4 mm wide and 3 mm thick. Measurements of dynamic Young's modulus (E) and damping (Q^{-1}) were conducted on each specimen using the piezoelectric ultrasonic composite oscillator technique (PUCOT) [8, 9] operating at a frequency of 120 kHz at temperatures ranging from room temperature to 622 °C. The changes in length and density of the specimen were taken into account for the high temperature analysis using the coefficient of thermal expansion for SiC [10].

4. Results and discussion

4.1. Microstructural observations

The micrographs of each specimen reveal that the microstructure was essentially isotropic. The phases were evenly distributed across the field of observation, and it was seen that both the longitudinal and transverse views were highly similar. Fig. 1 shows the optical micrograph of NC 203. From this micrograph, it can be seen that the microstructure is very uniform. The grey area, comprising the majority of the view, is SiC. The black areas are voids, and the white areas are sintering aids.

Figs 2 and 3 show the microstructures of RFSC No. 1 and RFSC No. 2. From these micrographs, it can be seen that the microstructure is uniform with very little porosity. The grey areas are SiC, while the white areas are Si, and the black areas are residual carbon. The phases in Fig. 3 are the same as those in Fig. 2, but the Si distribution is coarser. Figs 4 and 5 show the microstructures of RFSC No. 4 and RFSC No. 5. The grey areas in the micrographs are SiC, the white areas are Si, the dark brown/light brown areas are $MoSi_2$, and the black areas are residual carbon. The phases are evenly distributed throughout the sample, i.e. they are not concentrated around grain boundaries, or arranged as reinforcing "stringers". Fig. 5 shows a microstructure similar to that for RFSC No. 3, but there is more $MoSi_2$ present.

4.2. Comparison of properties at room temperature to ROM estimations

From Table II a comparison of the experimentally determined values of dynamic Young's modulus and

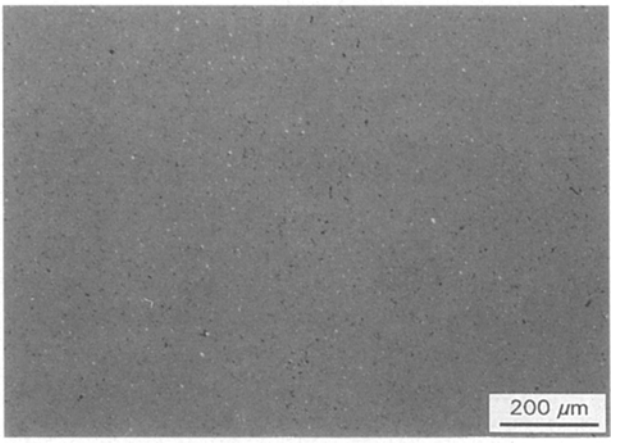

Figure 1 Optical micrograph of NC 203 (the grey area, comprising the majority of the view, is SiC; the black areas are voids, and the white areas are sintering aids).

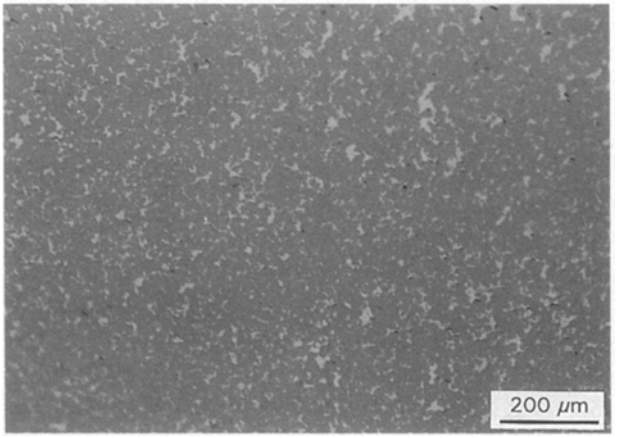

Figure 2 Optical micrographs of Si-infiltrated RFSC (the grey areas are SiC, the white areas are Si, and the black areas are residual carbon).

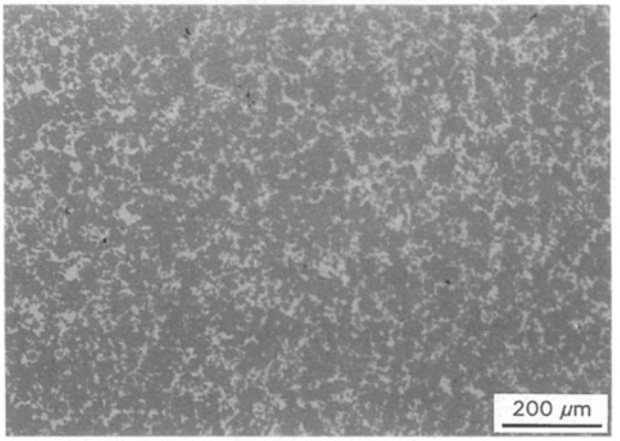

Figure 3 As Fig. 2 but the Si distribution is coarser.

density can be made with the "rule of mixtures (ROM)" estimations at room temperature for each specimen, calculated using published values for densities and Young's moduli [11–13].

From this comparison, it can be seen that there is a relatively high percentage difference for the elastic moduli in the reaction-formed specimens. The reason for this, in part, is that when the ROM calculations were made, it was assumed that the materials exhibited zero porosity, i.e. 100% theoretical density. There is also some uncertainty in the volume fractions of each phase, and the reactions governing the formation of each phase may not have carried on to completion. In addition, there is also some uncertainty since the bonding characteristics at the interface between phases are not known. Lastly, the modulus values used in the ROM calculations were obtained from published data. These modulus values may not reflect the actual modulus values of each phase in the material. Due to all the uncertainty, the ROM calculations can only be used to find a rough figure for the modulus range of RFSC. Regarding the ROM calculations for density, the percentage differences between the measured values of density and the ROM values are $< 5\%$ for four of the materials studied. However, for RFSC No. 4 the difference is somewhat higher, 12.1%. Some unreacted carbon might be responsible for the low value of measured density in this specimen. Thus, generally the ROM calculations for density can be used to find a fairly precise value for the density of RFSC.

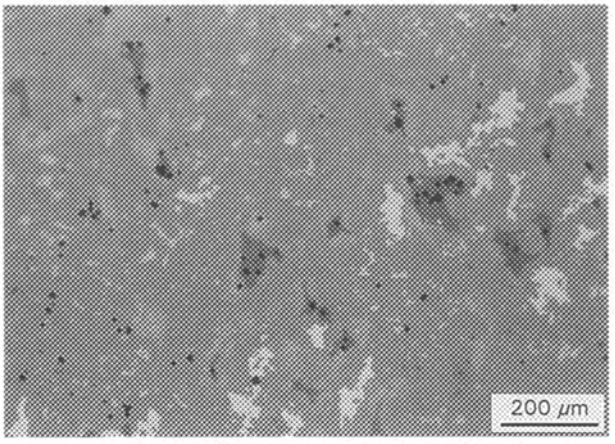

Figure 4 Optical micrograph of Si–Mo-infiltrated RFSC No. 4 (the grey areas are SiC, the white areas are Si, the dark brown/light brown areas are $MoSi_2$, and the black areas are residual carbon; the phases are evenly distributed throughout the sample, i.e. they are not concentrated around grain boundaries, or arranged as reinforcing "stringers").

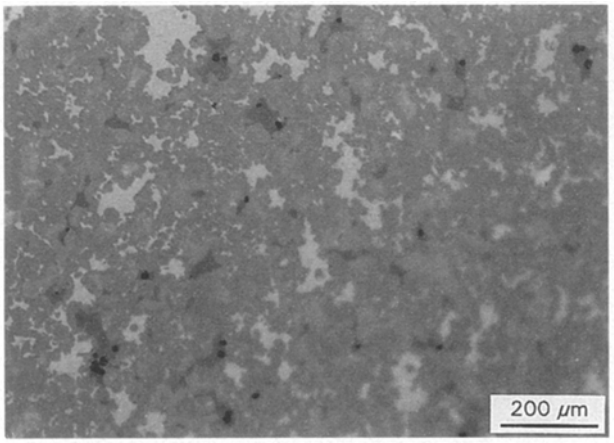

Figure 5 As Fig. 4 of RFSC No. 5.

4.3. Temperature dependency of the dynamic elastic modulus of RFSC

From Fig. 6 it can be seen that the dynamic Young's modulus of all samples decreases slightly as temperature increases. In each case, a linear regression was performed on the data to obtain the best fit. It was found that dynamic Young's modulus for each sample decreased linearly with increasing temperature. The best-fit equations are presented in Table III. Also included in Table III are the best-fit equations for the data shown in Fig. 7. [14, 15], which are included for comparison. The sample for curve A is a reaction-bonded SiC obtained from Coors Ceramics [14], while the material for curves B–D is α-SiC [15]. From Table III and Fig. 7 it can be seen that the fit for NC 203 is similar to the fits for Coors SiC and the α-SiC in that all fits exhibit a negative slope. However, the

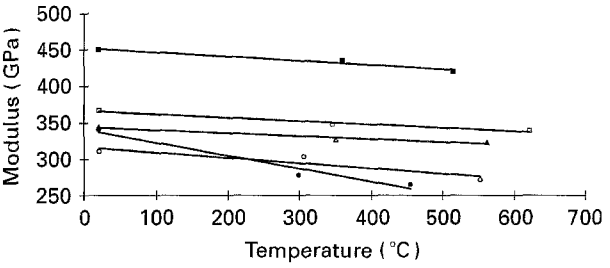

Figure 6 Dynamic Young's modulus versus temperature for SiC matrix materials. ■, NC 203; □, RFSC No. 1; △, RFSC No. 2; ●, RFSC No. 3; ○, RFSC No. 4.

TABLE II Comparison of ROM estimations with experimentally determined properties at room temperature

Specimen	ρ_{meas} (g cm^{-3})	ρ_{ROM} (g cm^{-3})	Diff. (%)	E_{meas} (GPa)	E_{ROM} (GPa)	Diff. (%)
NC 203[a]	3.328	3.17	4.8	450	470	4.4
RFSC No. 1	3.053	3.05	0.1	366	419	14.5
RFSC No. 2	2.955	3.05	3.2	344	419	21.8
RFSC No. 3	3.031	3.18	4.9	340	429	26.2
RFSC No. 4	2.945	3.30	12.1	310	438	41.3

[a] Calculated from published values of E and ρ for SiC, and accounting for porosity.

TABLE III Linear regression equations for E (GPa) versus T (°C) for SiC materials

Specimen	Linear regression	10^4 (Relative decrease) (K^{-1})
NC 203	$E = 452 - 0.0619T$	1.38
RFSC No. 1	$E = 366 - 0.0502T$	1.37
RFSC No. 2	$E = 344 - 0.0455T$	1.32
RFSC No. 3	$E = 340 - 0.1850T$	5.44
RFSC No. 4	$E = 316 - 0.0780T$	2.52
Coors SiC [14]	$E = 402 - 0.0143T$	0.36
α-SiC [15]	$E = 350 - 0.0153T$[a]	0.44

[a] Determined from Fig. 7.

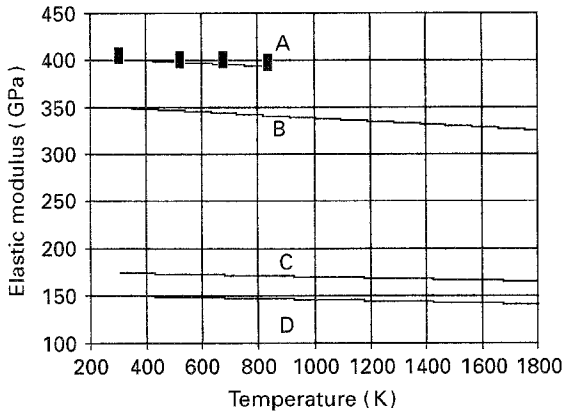

Figure 7 Curve A, dynamic Young's modulus versus temperature for Coors SiC [14]. Elastic moduli versus temperature for α-SiC [15]: curve B, Young's modulus; curve C, bulk modulus; curve D, shear modulus.

modulus is higher over the temperature range, and the slope for NC 203 is approximately four times the slopes for Coors SiC and α-SiC.

Also included in Table III is the relative decrease in dynamic Young's modulus of each specimen with increasing temperature. This was determined by normalizing the slope of the linear regression with respect to the modulus at room temperature. From Table III it can be seen that the relative decrease of modulus for SiC materials is very small. It can be seen that the relative decreases in the RFSC are higher than that for Coors SiC and α-SiC, but in the same range as that for the commercially produced SiC NC 203. This indicates that the reinforcing phases present in RFSC cause the relative decrease in modulus to be greater than that for pure α-SiC, but the values are still comparable to those of the NC 203 commercially produced SiC. It is to be noted that the values for relative decrease of modulus for all the SiC materials are generally lower than the values (4×10^{-4}–$14 \times 10^{-4}\ K^{-1}$) documented by Friedel [16] for pure elements (mainly metallic). This is probably a consequence of the predominant covalent bonding in SiC materials.

4.4. Damping characteristics

The strain amplitude dependence of damping is included for each specimen over temperature ranges as shown in Figs 8–12. From these graphs it can be seen that the damping for each specimen is generally independent of strain amplitude and is not affected greatly by temperature (over the range tested). For repetitive tests on a single specimen, the reproducibility of the value of damping was generally within a factor of 2–3. No large strain amplitude dependence of damping is expected in these ceramics, since the number of dislocations is expected to be small and the dislocations are not expected to move significantly at the temperatures used for the measurements.

The damping as a function of reciprocal temperature on a log-linear scale is shown in Fig. 13 and an Arrhenius plot has been fitted to the data. The

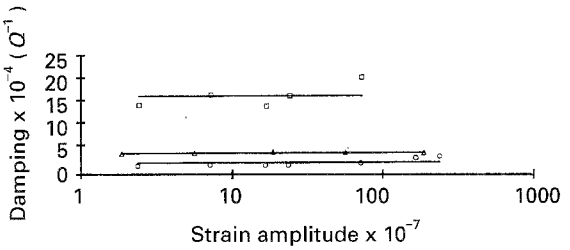

Figure 8 Strain amplitude dependence of damping for NC 203 at: △, 20; ○, 360; and □, 514 °C.

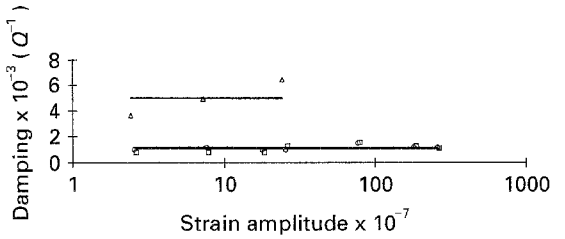

Figure 9 Strain amplitude dependence of damping for RFSC No. 1 at: △, 20; ○, 346; and □, 622 °C.

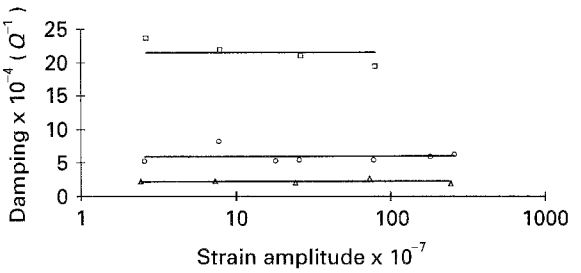

Figure 10 Strain amplitude dependence of damping for RFSC No. 2 at: △, 20; ○, 350; and □, 561 °C.

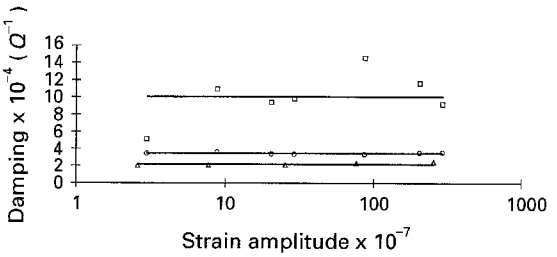

Figure 11 Strain amplitude dependence of damping for RFSC No. 3 at: △, 20; ○, 298; and □, 455 °C.

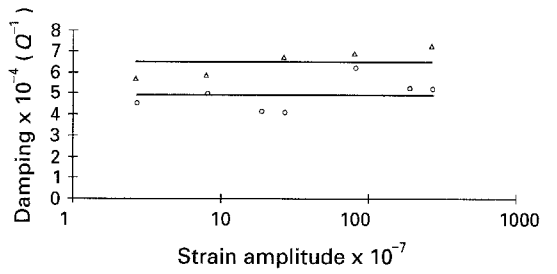

Figure 12 Strain amplitude dependence of damping for RFSC No. 4 at: △, 20; and ○, 305 °C.

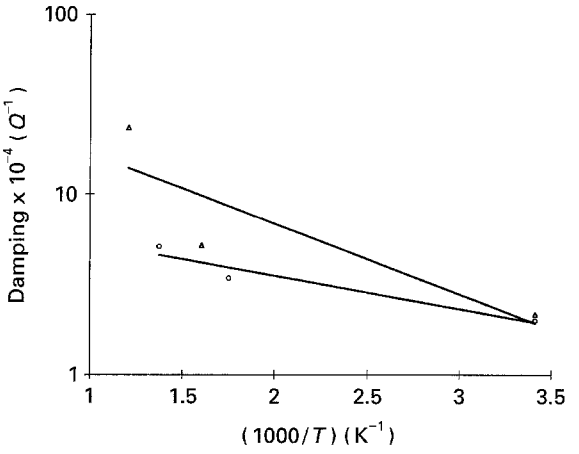

Figure 13 Damping versus reciprocal temperature for: △, RFSC No. 2; and ○, RFSC No. 3.

activation energy was determined for each specimen from:

$$Q^{-1} = Q^{-1}(0)\exp(-H/kT) \quad (1)$$

where Q^{-1} is the damping, $Q^{-1}(0)$ is a reference value of damping, H is the activation energy (in eV), k is the Boltzmann constant (8.61×10^{-5} eV K^{-1}) [13], and T is temperature (in K). The activation energy was determined for RFSC No. 2 and RFSC No. 3 only, since not enough damping data were obtained for the other specimens.

Table IV shows the values of the activation energy derived for specimens RFSC No. 2 and RFSC No. 3. By comparison, the activation energy for the diffusion of C in SiC is between 7.4 and 8.2 eV [17]. The activation energy determined for the RFSC materials was comparable to the thermal energy (kT) present across the temperature range used. Thus, for RFSC No. 2, kT was 0.025–0.072 eV, while for RFSC No. 3 kT was in the range 0.025–0.063 eV. Since the values of the activation energy derived from the damping data are close to the values for the thermal energy, and are also two orders of magnitude less than the activation energy for the diffusion of C in SiC, it can be deduced that damping due to crystal defect motion (dislocations, solute atoms, etc.) is not significant at the temperatures used.

TABLE IV Activation energies of SiC-based materials

Specimen	Activation energy (eV)
RFSC No. 2	0.08
RFSC No. 3	0.04
C in SiC [17]	7.4–8.2

4.5. Comparison of modulus and damping results to previously measured data [18, 19]

There is a limited amount of data available for modulus and damping characteristics of SiC materials. These characteristics will be compared to those results obtained from two other experiments in addition to the two previously mentioned studies. In the first experiment [18], SiC with B and C additives was studied from 0 to 1500 °C. In this study, several values of logarithmic decrement and square of frequency (f) of vibration in the torsional mode were plotted against temperature. Shear modulus (G) is proportional to f^2, and Young's modulus (E) for an isotropic material can be determined from:

$$E = 2G(1 + \nu) \quad (2)$$

where ν is Poisson's ratio (taken as 0.3 for SiC). The relative decrease in E was found by first normalizing the slopes of the f^2 curve with respect to the value of f^2 at room temperature, and then equating this to the relative decrease of shear modulus, and using this value in Equation 2. The damping was determined from:

$$Q^{-1} = \delta/\pi \quad (3)$$

where δ is the logarithmic decrement. An average value of the logarithmic decrement was determined from the scatter and then used to find the approximate value of Q^{-1}. The relative decrease in modulus was found to be 7×10^{-4} K^{-1}, which is a little higher than those values shown in Table III, but is still within the same order of magnitude. The damping was found to be ca. 2×10^{-3}, which corresponds to the same order of magnitude of damping measured for each specimen in this study.

The second experiment was an investigation of the elastic properties of SiC, AlN and their solid solutions [19]. From this study a comparison can be made between the measured value of Young's modulus for pure SiC with a porosity of ca. 0.013 v/o, which was 427 GPa, and our NC 203 (which has a similar porosity). The measured value for the modulus of NC 203 was 450 GPa. Thus, the agreement is within ca. 5%.

5. Conclusions

From these studies of the microstructure and the elastic and anelastic properties of RFSC, it is concluded that:

1. the microstructure of RFSC are essentially isotropic with a uniform distribution of phases;
2. "rule of mixtures" calculations cannot be used to predict accurately the elastic modulus of RFSC;
3. "rule of mixtures" calculations can be used to predict the density of RFSC to within ca. 5%;
4. the dynamic Young's modulus of RFSCs decreases from ca. 350 to 300 GPa as temperature increases from room temperature to 600 °C;
5. the characteristics of Young's modulus versus temperature are similar to those of other SiC materials;
6. the relative slopes of Young's modulus versus temperature of the RFSC are higher than those of Coors SiC and pure α-SiC, but similar to that of the commercially produced NC 203 SiC material;
7. the damping of RFSC is independent of strain amplitude and is not greatly affected by temperature up to 600 °C.

Acknowledgements

The authors appreciate the metallographic assistance of Scott Cronauer and Tom Stephens, and valuable discussions, with Drs H. R. Thornton and A. J. Giacomin.

References

1. E. FITZER and R. GADOW, *Amer. Ceram. Soc. Bull.* **65** (1986) 325.
2. P. J. LAMICQ, G. A. BERNHART, M. M. DAUCHIER and J. G. MACE, *ibid.* **65** (1986) 336.
3. M. E. WASHBURN and W. S. COBLENZ, *ibid.* **67** (1988) 356.
4. D. R. BEHRENDT and M. SINGH, *J. Mater. Syn. Process.* **2** (1994) 133.
5. M. SINGH, R. PAWLIK, J. A. SALEM and D. R. BEHRENDT "Advances in ceramic matrix composites" (The American Ceramics Society, Westerville, OH, 1993). 349.
6. M. SINGH and D. R. BEHRENDT, *Mater. Sci. Engng.* **A194** (1995) 193.
7. *Idem.* NASA Technical Memorandum 105860 (1992).
8. J. MARX, *Rev. Sci. Instrum.* **22** (1951) 503.
9. W. H, ROBINSON and A. EDGAR, "IEEE, Transactions on sonics and ultrasonics", Su-[9]21, **2** (American Institute of Electrical and Electronic Engineers 1974) p. 98.
10. J. F. SHACKELFORD, "Introduction to materials science for engineers" (Macmillan, New York 1985) p. 324.
11. F. E. BACON, "Properties of silicon: Metals handbook", 8th Ed, Vol. 1 (ASM Int., Metals Park, OH, 1966).
12. J. Z. BRIGGS, "Properties of molybdenum: Metals handbook" 8th Ed, Vol. 1 (ASM Int., Metals Park, OH, 1966).
13. L. H. VAN VLACK, "Elements of materials science and Engineering", 4th Ed, (Addison-Wesley, Reading, MA, 1980).
14. P. T. JAMINET, A. WOLFENDEN and V. K. KINRA, in "Damping and dynamic elastic modulus of ceramics and ceramic–matrix composites at elevated temperatures, M^3D: Mechanics and mechanisms of material damping" (ASTM, STP 1169, Philadelphia, PA, 1992) p. 431.
15. M. FUKUHARA and Y. ABE, *J. Mater. Sci. Lett.* **12** (1993) 681.
16. J. FRIEDEL, "Dislocations" (Pergamon Press, New York, 1964) Appendix B, p. 454.
17. J. D. HONG and R. F. DAVIS, *J. Amer. Ceram. Soc.* **63** (1980) 546.
18. K. NISHIYAMA, M. YAMANAKA, M. OMORI and S. UMEKAWA, *J. Mater. Sci. Lett.* **9** (1990) 526.
19. R. RUH, A. ZANGVIL and J. BARLOWE, *Amer. Ceram. Soc. Bull.* **64** (1985) 1368.

Received 29 June 1994
and accepted 5 April 1995